

11/11

12
BS

NOSC

NOSC TD 447

NOSC TD 447

Technical Document 447

GHz ANALOG FIBER OPTIC REPEATER FOR RADAR MTI

CT Chang

15 June 1981

Prepared for
Naval Sea Systems Command

AD A102601

DTIC FILE COPY

DTIC
SELECTED
AUG 14 1981

A

Approved for public release; distribution unlimited

NAVAL OCEAN SYSTEMS CENTER
SAN DIEGO, CALIFORNIA 92152

81 8 14 0 42



NAVAL OCEAN SYSTEMS CENTER, SAN DIEGO, CA 92152

AN ACTIVITY OF THE NAVAL MATERIAL COMMAND

SL GUILLE, CAPT, USN
Commander

HL BLOOD
Technical Director

ADMINISTRATIVE INFORMATION

Work was done under program element 62712N, subproject SF12141491, by Optical Electronics Branch (Code 9225). The project was managed by JH Maynard, Head, Command Control-Electronic Warfare Systems and Technology Department; and work was performed for the NAVSEA Radar Block Program which is funded by Naval Sea Systems Command, C Jedrey (NSEA 62R13).

Released by
HH Wieder, Head
Electronic Material
Sciences Division

Under authority of
PC Fletcher, Head
Electronics Engineering
and Sciences Department

Accession For	
CONFIDENTIAL	<input checked="" type="checkbox"/>
RESTRICTED	<input type="checkbox"/>
Unannounced	<input type="checkbox"/>
Justification	
Distribution/	
Availability Codes	
Dist	Special
A	

111 NOV 17 1981

UNCLASSIFIED

SECURITY CLASSIFICATION OF THIS PAGE (When Data Entered)

REPORT DOCUMENTATION PAGE		READ INSTRUCTIONS BEFORE COMPLETING FORM
1. REPORT NUMBER NOSC Technical Document 447 (TD 447)	2. GOVT ACCESSION NO. AD-A102601	3. RECIPIENT'S CATALOG NUMBER
4. TITLE (and Subtitle) GHZ ANALOG FIBER OPTIC REPEATER FOR RADAR MTI	5. TYPE OF REPORT & PERIOD COVERED Final	
7. AUTHOR(s) CT Chang	6. PERFORMING ORG. REPORT NUMBER	
9. PERFORMING ORGANIZATION NAME AND ADDRESS Naval Ocean Systems Center San Diego, CA 92152	8. CONTRACT OR GRANT NUMBER(s) N715044	
11. CONTROLLING OFFICE NAME AND ADDRESS Naval Sea Systems Command Washington, DC 20362	10. PROGRAM ELEMENT, PROJECT, TASK AREA & WORK UNIT NUMBERS 62712N, SF12141491 17	
14. MONITORING AGENCY NAME & ADDRESS (if different from Controlling Office)	12. REPORT DATE 15 Jun 1981	
	13. NUMBER OF PAGES 18	
	15. SECURITY CLASS. (of this report) Unclassified	
	15a. DECLASSIFICATION/DOWNGRADING SCHEDULE	
16. DISTRIBUTION STATEMENT (of this Report) Approved for public release; distribution unlimited		
17. DISTRIBUTION STATEMENT (of the abstract entered in Block 20, if different from Report)		
18. SUPPLEMENTARY NOTES		
19. KEY WORDS (Continue on reverse side if necessary and identify by block number) Delay lines Target position indicators Fiber optics Moving targets - Low flying Optical materials Radar equipment - Repeaters MICROWAVE FIR		
20. ABSTRACT (Continue on reverse side if necessary and identify by block number) A 0.85(um) fiber optic repeater is assembled and characterized. It consists of an avalanche photodiode receiver, a wideband amplifier, and a laser diode transmitter. Characteristics investigated include pulse fidelity, dynamic range, noise figure, and frequency response. Good agreement between measurement and prediction is obtained for dynamic range and noise figure.		

DD FORM 1473 1 JAN 73

EDITION OF 1 NOV 65 IS OBSOLETE
S/N 0102-LF-014-6601

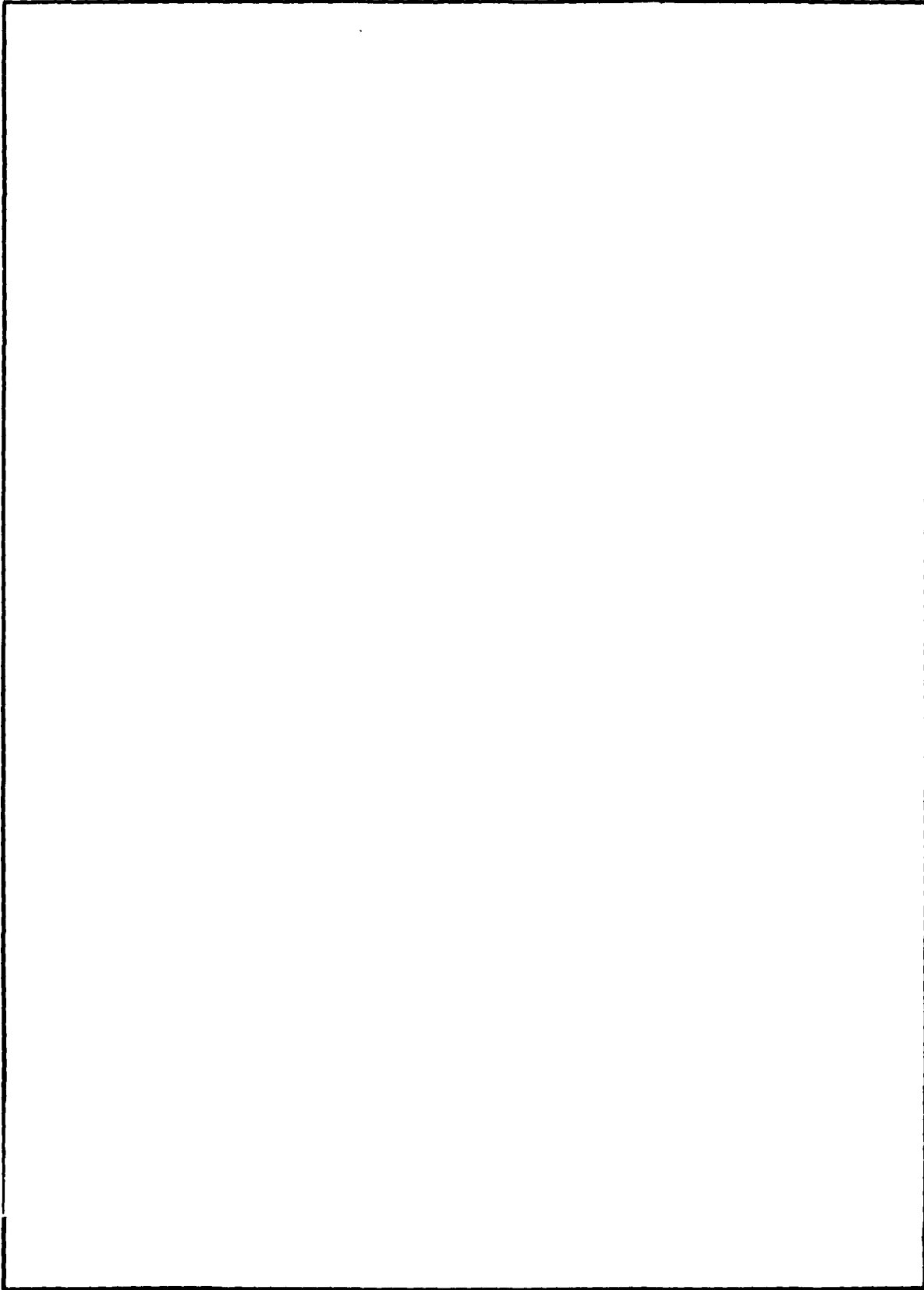
UNCLASSIFIED

SECURITY CLASSIFICATION OF THIS PAGE (When Data Entered)

392154

UNCLASSIFIED

SECURITY CLASSIFICATION OF THIS PAGE (When Data Entered)



UNCLASSIFIED

SECURITY CLASSIFICATION OF THIS PAGE (When Data Entered)

INTRODUCTION

To avoid the multipath propagation effects due to reflection from the sea surface, shipboard radar must be operated at a high frequency (such as K band) for the detection of low flying targets. However, a conventional coherent moving-target indicator (MTI) is difficult to operate at such a high frequency¹. An alternate approach is a noncoherent MTI based on subtraction of radar returns from two successive pulses, using a fiber optic delay line as a delay medium. This pulse-to-pulse subtraction will retain the moving target signal returns and reject the stationary clutter returns. A radar pulse of 1-ns width (after pulse compression) and 1-ms separation (pulse repetition interval) can detect low flyers with radial speed greater than about 500 ft/s (1 ft/s = 0.3048 m/s).

The required fiber optic delay line length is 200 km for 1-ms delay. Only fiber optic delay lines appear to have the real-time capacity for preserving the 1-ns pulse after 1-ms delay. Because of finite fiber attenuation (~ 2.5 dB/km at 0.85 μ m), it is impossible to transmit a 1-ns pulse over such a long fiber. Thus, a GHz analog fiber optic repeater is needed to strengthen the optical pulse amplitude during its transmission. This repeater consists of an avalanche photodiode (APD) receiver, a wideband amplifier, and a laser diode transmitter.

A weak input optical pulse is detected by the APD receiver and amplified. The amplified pulse is used to drive the transmitter to generate a strong output optical pulse. Repeater performance characteristics pertaining to the radar MTI application are investigated. These include pulse fidelity, linearity, dynamic range, noise figure, and frequency response. Good agreement between experimental measurements and analytical predictions is obtained on the repeater dynamic range and repeater noise figure.

EXPERIMENTAL CHARACTERIZATION OF THE REPEATER

The repeater consists of an avalanche photodiode (APD) receiver R, a cascaded amplifier A, and a laser diode transmitter T as shown in fig 1. A weak input optical pulse is detected and amplified. The amplified electrical pulse in turn is used to drive the laser diode transmitter T to generate a strong output optical pulse. The APD receiver R has a quantum efficiency of approximately 60% and a frequency bandwidth from dc to 3.5 GHz. The avalanche gain M, defined as the ratio of avalanche photocurrent to primary photocurrent, is measured to be $M = 39$. The avalanche photocurrent 136 μ A is obtained from the dc voltage 6.8 mV developed by the receiver across the 50 Ω input impedance of the oscilloscope (Tektronix 7104 with GHz real-time

1. CT Chang, DE Altman, DR Wehner, and DJ Albares, Noncoherent Radar Moving Target Indicator Using Fiber Optic Delay Lines, IEEE Trans Ckt and Sys CAS-26, 1132-1135 (1979)

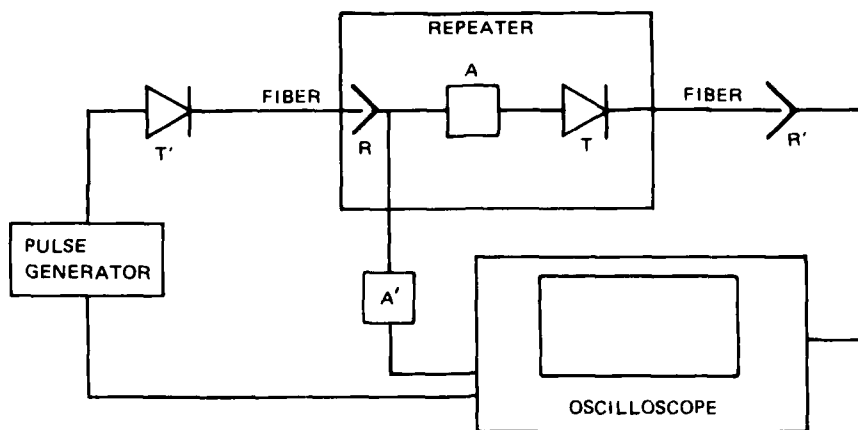
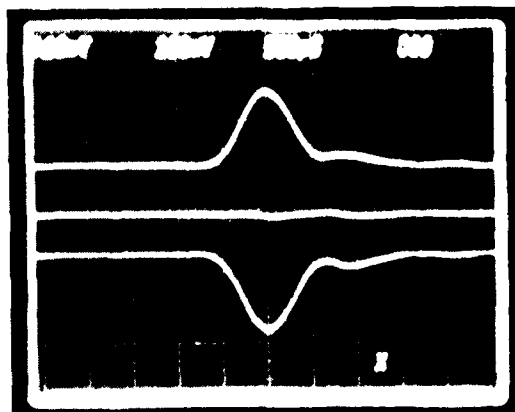


Figure 1. Block diagram of the experimental set up for a GHz analog fiber repeater. This repeater consists of an APD receiver R, a cascaded amplifier A, and a laser diode transmitter T.

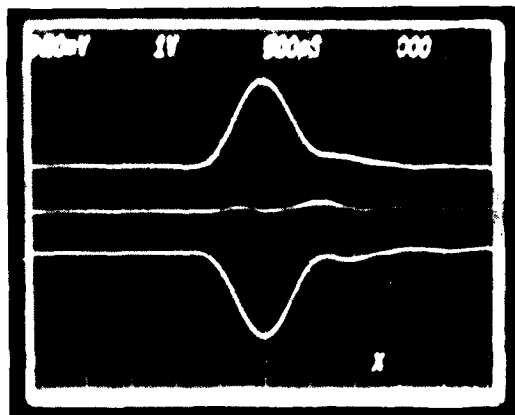
capacity), while the primary photocurrent of $3.49 \mu\text{A}$ is estimated from the dc (biasing) optical power of $8.51 \mu\text{W}$ and the APD responsivity $r = 0.41 \text{ A/W}$ for the primary photocurrent generation. The amplifier used in the repeater is composed of Walkins-Johnson models 6023-327 and 6023-432 cascaded together, with 6023-432 as the output stage. This cascaded amplifier provides 50-dB gain. The real-time pulse responses of the two amplifiers are shown in fig 2, with input and output pulses as top and bottom traces, respectively. The fidelity of the amplifier is shown as the central trace. This trace is the difference between input and output pulses. The transmitter T is the General Optronics laser diode GOLT-3 pigtailed with a single-mode optical fiber. The static light vs current (L-I) curve is shown in fig 3. The dc biasing current of the laser is 70 mA, while the lasing threshold is approximately 64 mA. This biasing above the lasing threshold is necessary in order to obtain a subnanosecond laser response for use in the GHz analog fiber optic repeater.

In order to evaluate the repeater performance, additional laser transmitter T' and the APD receiver R' are utilized for generation of the repeater input optical pulses and for detection of the repeater output optical pulses, respectively (see fig 1). The transmitter T' is biased above its lasing threshold and is then driven by a current pulse from the pulse generator. Both biasing current and pulsing current are fixed during the experimental characterization of the repeater. The ratio between pulsed optical power P and biasing (dc) optical power P_b is measured to be

$$\frac{P}{P_b} = 1.35 .$$



(a) pulse response of the
Walkins-Johnson Amplifier 6023-327



(b) pulse response of the
Walkins-Johnson Amplifier 6023-432

Figure 2. Pulse responses of the amplifier: input and output pulses are shown as the top and bottom traces, respectively. The difference between input and output pulses is the central trace.

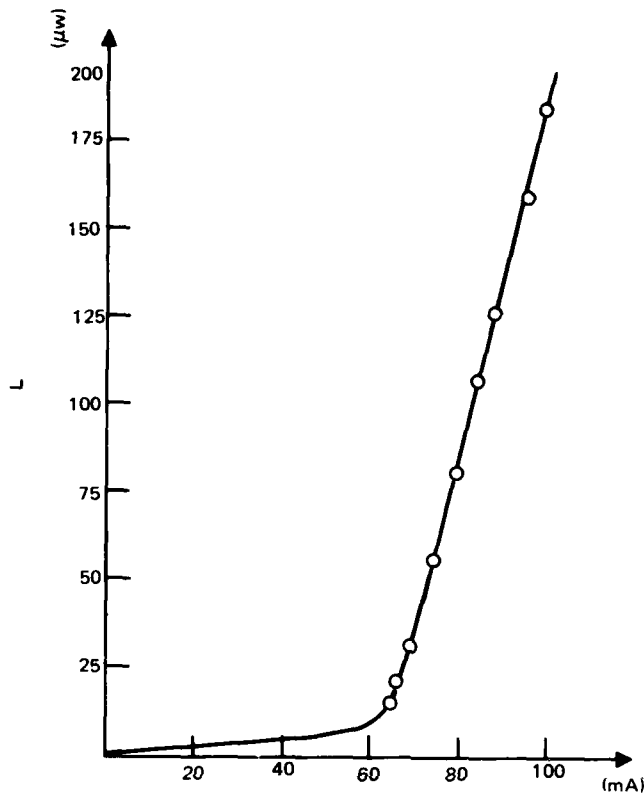


Figure 3. Static light vs current characteristics for the General Optronics laser diode GOLT-3 pigtailed with a single mode optical fiber.

This ratio is obtained by observing the detected input optical pulse displayed over the oscilloscope in the dc coupling mode. The avalanche gain of the APD receiver R' is measured to be $M' = 45.1$ under similar measurement procedures described previously.

Typical pulse responses of the repeater are shown in fig 4. Here the top trace is the detected input optical pulse amplified by the amplifier A' with 30-dB gain and the bottom trace is the detected output optical pulse. The central trace shows the difference, indicating the fidelity of the repeater is such that the pulse amplitude difference is typically 20 dB down as compared to the input or output pulses. The repeater (electrical) gain is approximately 30 dB.

The repeater linearity is shown in fig 5. Various input and output levels are obtained by changing the repeater input optical coupling between T' and R. This simulates input optical pulses under various optical fiber attenuations before their arrivals at the repeater. This repeater is linear from 1.8 to 215 mV. Here, 1.8 mV is the minimum detectable output pulse with

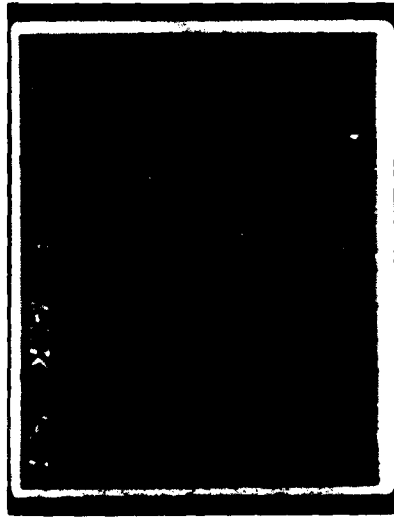
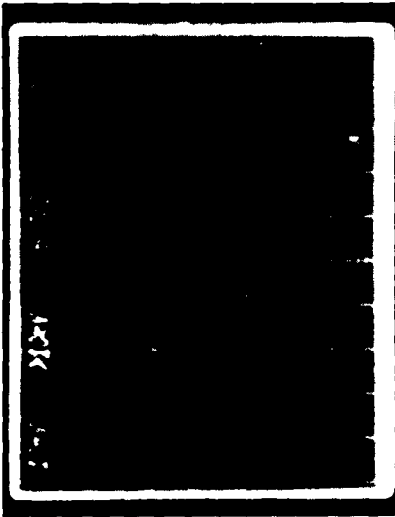
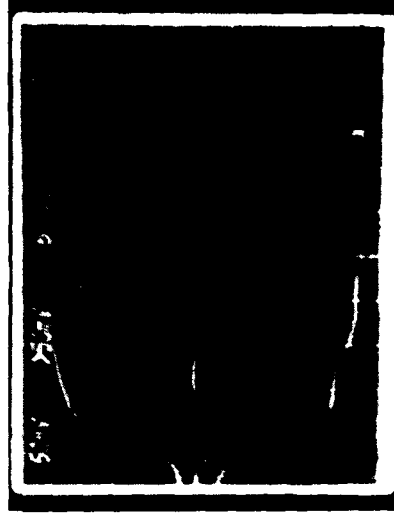
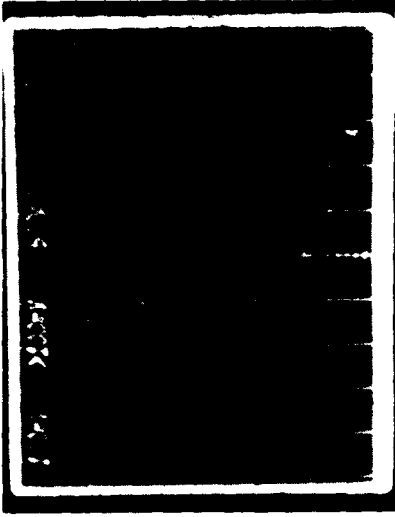


Figure 4. Various pulse responses of the repeater. Top trace is the detected (by R) input optical pulse after 30-dB amplification, while the bottom trace is the detected (by R') output optical pulse. The central trace is the difference between input and output pulses. The electrical gain of the repeater is 30 dB, while the optical gain is about 15 dB.

$(S/N)_o = 1$, and 215 mV is the maximum output pulse with 3-dB compression in the repeater gain.

The signal to noise ratios of the input pulses $(S/N)_i$ and the output pulses $(S/N)_o$ are measured by assuming the noise to be Gaussian distributed. The Gaussian noise is measured by the tangential method².

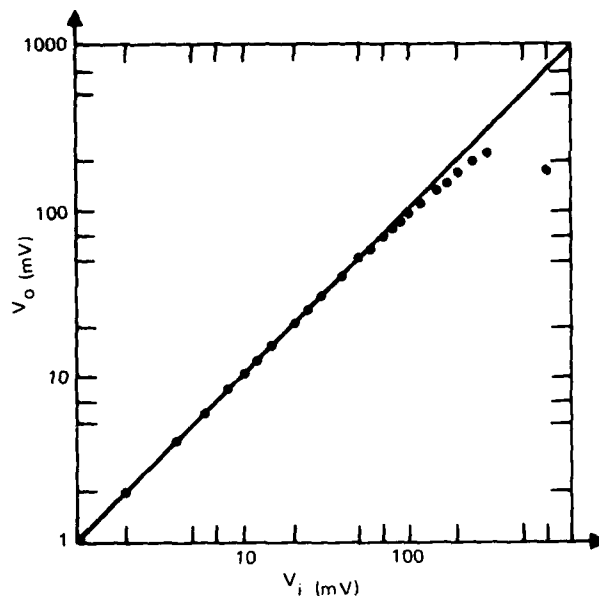


Figure 5. Repeater output amplitude (V_o) vs repeater input amplitude (V_i). This figure shows the repeater linearity.

- a. The detected optical pulse is equally split and then ac coupled to both channels of the 7104 oscilloscope used in the alternate-sweep mode.
- b. The offset voltage of one channel is adjusted until these two identical pulses form a combined trace that has a uniform intensity distribution over its central portion.
- c. The noisy pulses are then removed. The difference in the noise-free traces is twice the rms noise voltage 2σ .
- d. The signal to noise ratio in dB is

2. G Franklin and T Hatley, Don't Eyeball Noise, Elec Dsgn, 24, 184-187 (1973)

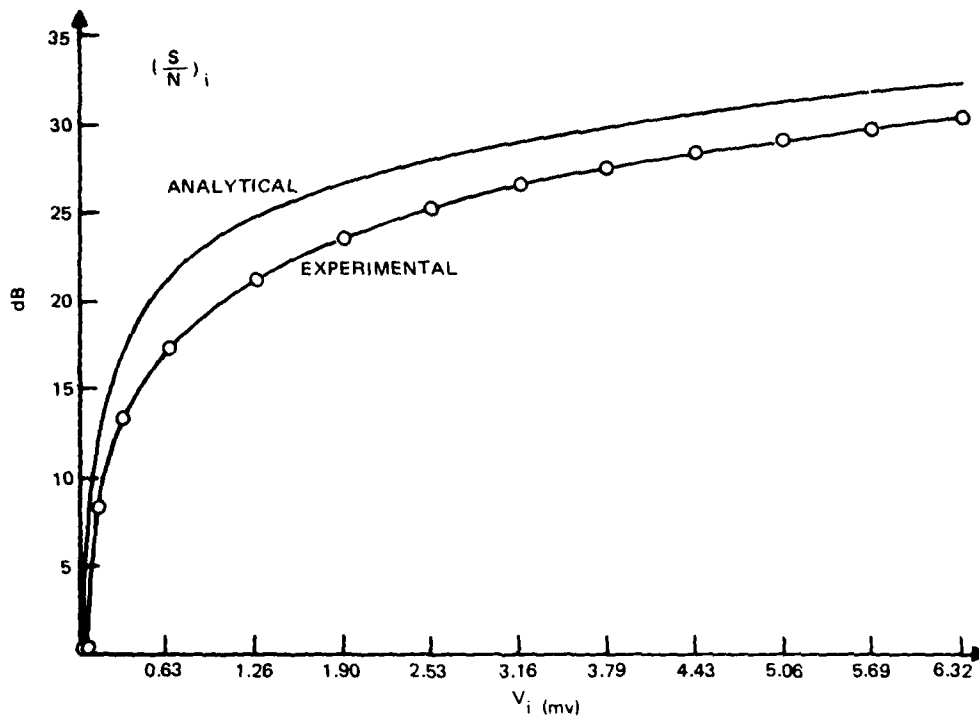


Figure 6. Input signal (or pulse amplitude) to noise ratio $(\frac{S}{N})_i$ as a function of input pulse amplitude V_i . The measured $(\frac{S}{N})_i$ includes the noise contribution from the amplifier A' (see fig 1). The real repeat $(\frac{S}{N})_i$ without noise contribution from the amplifier A' should be approximately 4 dB higher than that shown in in this figure.

$$(\frac{S}{N}) = 20 \log_{10} \frac{V_p}{\sigma}$$

where V_p is the detected optical pulse amplitude. This tangential method relies on the fact that two identical Gaussian distributed curves just form a single curve with no dips in trace intensity (or uniform intensity), when the curves are separated by exactly two times rms noise voltage (2σ). The point at which this occurs is independent of the height of the curves, the length of observation, or the scope intensity.²

The measured repeater input signal to noise ratio $(S/N)_i$ as a function of the input pulse amplitude is shown in fig 6, while the corresponding

repeater output signal to noise ratio $(S/N)_o$ is shown in fig 7. The noise figure for the repeater, indicating the ratio of $(S/N)_i$ to $(S/N)_o$, is shown

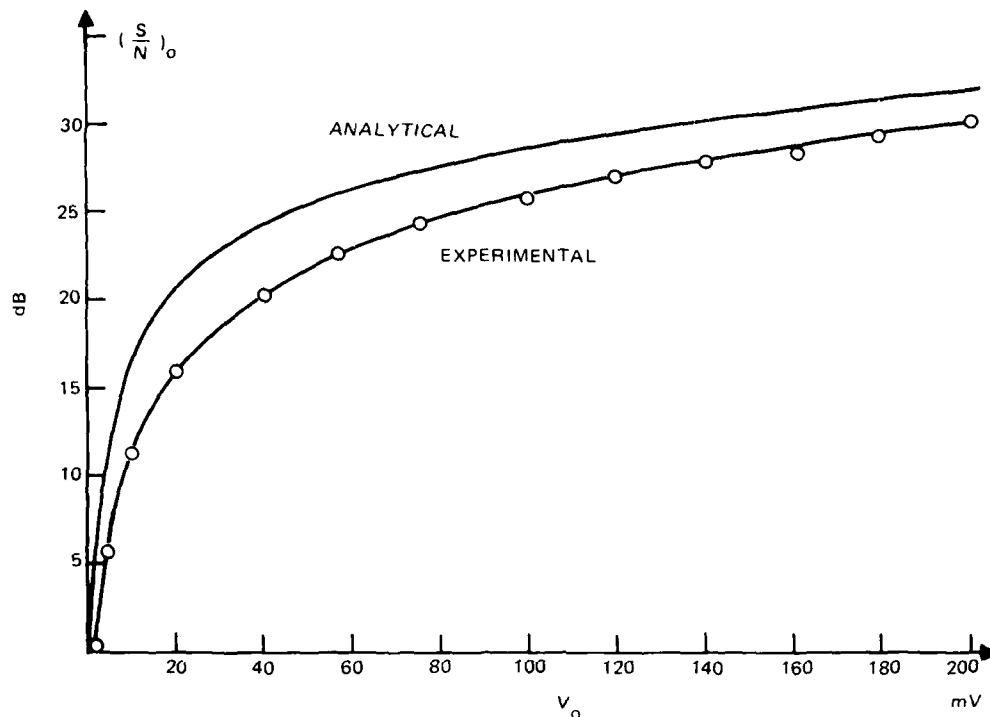


Figure 7. Output signal (or pulse amplitude) to noise ratio $(\frac{S}{N})_o$ as a function of output pulse amplitude V_o .

in fig 8. The input noise in figs 6 and 8 includes both the input repeater noise and the noise generated by the amplifier A'. The amplifier A' is needed because the input pulse without amplification is weak and is not suitable for the measurement of input signal to noise ratio over the oscilloscope. Assuming the amplifier A' has a noise figure of 4 dB, then the measured repeater $(S/N)_i$ and noise figure should be 4 dB up in figs 6 and 8.

The frequency response of the repeater consisting of the amplifier A, transmitter T, and receiver R' is shown in fig 9. This frequency response is linear within +2 dB from 10 MHz to 1.3 GHz. The laser biasing is set to be 80 mA so that the laser is never operating below its lasing threshold during the process of swept frequency measurement using an HP spectrum analyzer.

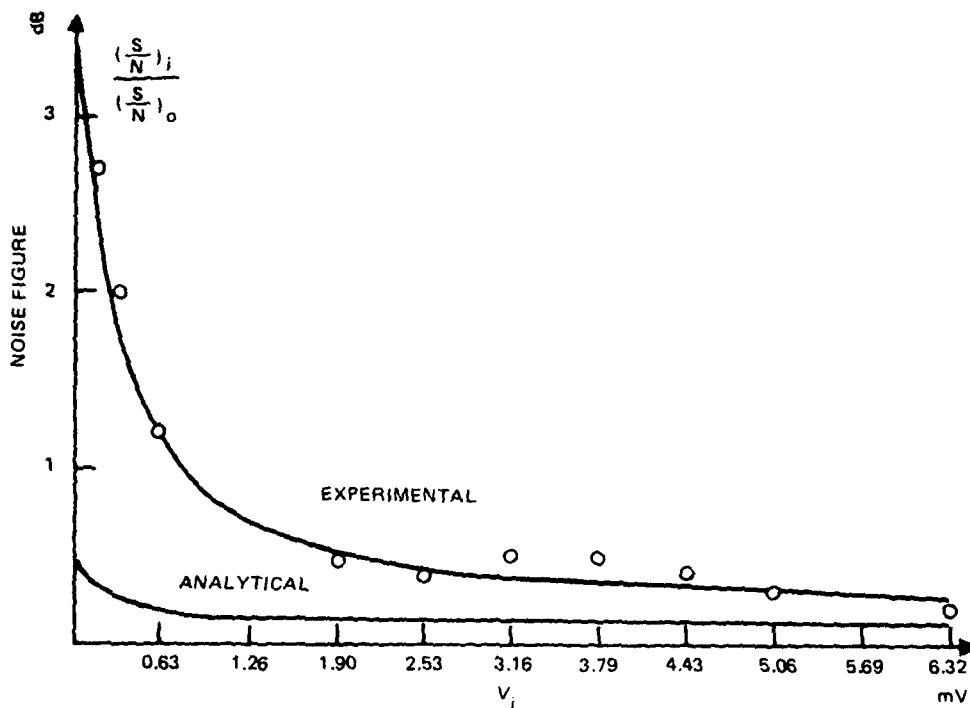


Figure 8. Repeater noise figure (NF) as a function of input pulse amplitude V_i . The measured noise figure shown includes the noise contribution from the amplifier A'. The real repeater NF should be approximately 4 dB higher than the measured NF shown in the figure.

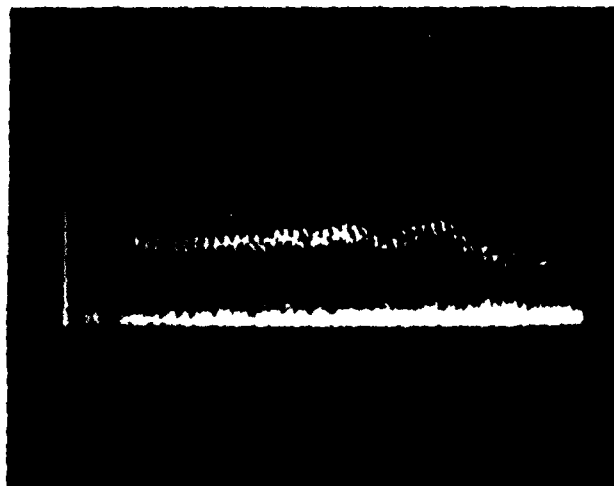


Figure 9. Frequency response of the repeater from 10 MHz to 2 GHz. One vertical division corresponds to 10 dB.

ANALYSIS OF THE REPEATER PERFORMANCE

The APD receiver is used for the detection of input optical pulses, because the system described in fig 1 is a 50Ω system. This APD receiver provides avalanche gain without much degradation in S/N, since the thermal noise associated with 50Ω is the dominant noise. Both photodetection and avalanche gain are random processes and contribute to the excess noise. This excess noise³ can be characterized by a noise factor.

$$F(M) = kM + \left(2 - \frac{1}{M}\right) (1 - k), \quad (1)$$

where M is the avalanche gain and k is the carrier ionization ratio. Let r be the responsivity in A/W for the generation of primary photoelectrons and e the electron charge; then the mean square shot noise current³ associated with the photodetection using an APD receiver is

$$\langle i_q^2 \rangle = 2 e F(M) M^2 r (P_b + P) B. \quad (2)$$

Here P and P_b are pulsed optical power and dc biasing optical power, respectively. The notation B represents the overall bandwidth for detection and display of the optical pulses. The bandwidth of this system is limited to $B = 10^9$ Hz, by the GHz real-time oscilloscope (Tektronix 7104). Both oscilloscope and amplifier have an input impedance $R_i = 50\Omega$. Thermal fluctuation of the photocurrent across the 50Ω input impedance contributes to the mean square thermal noise current,

$$\langle i_t^2 \rangle = \frac{4KTB}{R_i} = (5.7 \times 10^{-7} \text{ A})^2. \quad (3)$$

The thermal fluctuation energy KT is evaluated at room temperature ($T = 295\text{K}$) in eq (3).

The signal photocurrent i_s of the detected optical pulse is

$$i_s = M r P. \quad (4)$$

Combining eqs (2), (3), and (4), we find the signal to noise ratio for detection of optical pulse power P superimposed on a dc biasing power P_b is

3. RG Smith and SD Personick, in Semiconductor Devices for Optical Communication, ed by H Kressel (Springer-Verlag, New York, 1979), ch 4

$$\frac{S}{N} = \frac{(MrP)^2}{2eF(M) M^2 r (P+P_b) B + \frac{4kTB}{R_i}} \quad (5)$$

The dark current ($\sim 10^{-9}$ A) of the APD receiver is neglected in eq (5) since its contribution to the shot noise is small compared to the thermal noise in eq (3).

Now we apply eq (5) to the APD receiver R with primary photoelectron responsivity $r = 0.41$ A/W. This APD receiver has an avalanche gain $M = 39$ and an excess avalanche noise factor $F(M) = 3.27$ obtained by assuming the carrier ionization ratio³ $k = 0.035$ in eq (1). Putting these characteristics of the receiver R, eq (3), and the measured relationship $P_{bi} = 1/1.35 P_i$ into eq (5), we obtain $(S/N)_i$ for the detected input optical pulse generated by the transmitter T':

$$\left(\frac{S}{N}\right)_i = \frac{(16P_i)^2}{1.14 \times 10^{-6} P_i + 3.25 \times 10^{-13}} \quad (6)$$

The numerator in eq (6) is the input signal current $i_s = 16 P_i$. This input signal displayed over the oscilloscope becomes input signal voltage:

$$V_i = 799.5 P_i \quad (7)$$

Figure 6 shows the input signal to noise ratio $(S/N)_i$ from eq (6) as a function of input signal voltage V_i from eq (7). This analytical curve is in reasonable agreement with the corresponding measured curve.

The repeater has an experimentally measured gain of 30 dB (voltage gain of 31.6), as shown in fig 5. Thus, the repeater output pulse voltage displayed over the oscilloscope will be

$$V_o = 31.6 \times 799.5 P_i = 25264 P_i \quad (8)$$

The APD receiver R' has a measured avalanche gain $M' = 45.1$ and its responsivity for primary photocurrent is assumed to be $r' = 0.41$ A/W. Therefore, the pulsed optical power from the transmitter T will be

$$P_o = \frac{V_o}{(45.1 \times 0.41) \times 50} = 27.3 P_i \quad (9)$$

This means that the optical power gain of the repeater is 27.3. This optical gain is different from the measured voltage gain of 31.6 because of different avalanche gains between the receivers R and R'.

The output optical pulse generated by the transmitter T consists of a pulsed optical power P_o superimposed on a $38\text{-}\mu\text{W}$ dc optical power. The APD receiver R' used for the detection of this output optical pulse has an excess noise factor $F(M') = 3.49$. This excess noise factor is obtained from eq (1) with $M' = 45.1$ and $k' = 0.035$. Thus, the signal to noise ratio $(S/N)_o$ for the detected output optical pulse is

$$\left(\frac{S}{N}\right) = \frac{(18.5 P_o)^2}{9.3 \times 10^{-17} (P_o + 3.8 \times 10^{-5}) + (1.14 \times 10^{-6} P_i + 3.25 \times 10^{-13}) \times 1000} \quad (10)$$

The first term in the denominator is the shot noise and excess noise (see eq (2)) associated with the output photodetection using the APD receiver R', while the second term is the input shot noise associated with the receiver R and the 50Ω input resistance of the amplifier A amplified by the 30-dB repeater gain. The repeater output $(S/N)_o$ from eq (10) as a function of the repeater output voltage V_o from eq (8) is shown in fig 7. The difference in dB between figs 6 and 7 is shown in fig 8. This is the analytical noise figure of the repeater.

DISCUSSION

The repeater dynamic range is defined as the ratio of maximum output optical pulse to the minimum detectable optical pulse. The minimum detectable optical pulse is obtained by letting eq (10) equal 1 and then solving it for P_o with the aid of eq (9). The result is $P_{o \min} = 1 \mu\text{W}$. This implies the minimum detectable output optical pulse displayed over the oscilloscope to be $V_{o \min} = 0.95 \text{ mV}$. This analytical prediction is to be compared with the measured value $V_{o \min} = 1.7 \text{ mV}$ or $P_{o \min} = 1.8 \mu\text{W}$. Thus, the repeater dynamic range D is

$$D = \begin{cases} 20 \log_{10} \left(\frac{300}{0.95}\right) = 50 \text{ dB} & \text{(analytical)} \\ 20 \log_{10} \left(\frac{215}{1.7}\right) = 42 \text{ dB} & \text{(experimental),} \end{cases}$$

where 215 mV is the maximum output optical pulse amplitude displayed over the oscilloscope (see fig 5) and 300 mV is the theoretical maximum output pulse if the repeater is perfect without gain compression. The maximum optical pulse is found to be limited by the amplitude of the optical pulse generated by the laser diode transmitter T as well as by the coupling efficiency between the transmitter T and its pigtailed single-mode optical fiber. The minimum detectable optical pulse is mainly limited by the repeater noise, as shown in the denominator of eq (10). Two important mean square noise currents at the repeater output are:

(1) The thermal noise associated with the 50Ω input resistance of the amplifier A:

$$\langle i_t^2 \rangle = (3.25 \times 10^{-13} \times 1000) = 3.25 \times 10^{-10} \text{ A}^2 .$$

(2) The shot noise associated with the photodetection of the dc biasing optical power of $38 \mu\text{W}$ from the transmitter T:

$$\langle i_q^2 \rangle = 3.5 \times 10^{-11} \text{ A}^2 .$$

Thus, the dominant repeater noise is the thermal noise associated with the 50Ω input resistance of the 50-dB amplifier.

The slope of the static L-I curve for the transmitter T at the driving current above the lasing threshold obtained from fig 3 is

$$\frac{dL}{dI} = 5 \frac{\mu\text{W}}{\text{mA}} .$$

If the input optical pulse P_i is detected by the receiver R with primary responsivity 0.41 A/W and avalanche gain 39, then the photocurrent will be $P_i \times (0.41 \times 39)\text{A}$. The photocurrent is amplified by an amplifier with voltage gain of 316 (50 dB). This amplified pulse is then driving the laser transmitter T with $\frac{dL}{dI} = 5 \times 10^{-3} \text{ W/A}$. Thus, the output optical P_o will be

$$\begin{aligned} P_o &= P_i \times (0.41 \times 39) \times 316 \times 5 \times 10^{-3} \\ &= 25.3 P_i . \end{aligned}$$

This implies that the repeater has an optical gain 25.3 based on the static L-I curve in fig 3. This gain is less than the 27.3 obtained from the experimental measurement. The difference probably is the direct result of the difference between static and dynamic L-I curves. The typical optical pulse used in this experiment has 1-ns pulse width and 3- μs pulse separation. This low duty pulse (with <1% duty) makes $\frac{dL}{dI}$ large for the dynamic L-I curve,

since the thermal effect due to pulsing current is negligibly small in this low duty pulse operation.

The typical problems encountered in the evaluation of this GHz analog fiber optic repeater are laser relaxation oscillation and laser self-pulsation (see fig 10 and 11). Both cause appreciable difference between input and output repeater pulses. This then makes the task of the analog repeater difficult. Another problem typically encountered is laser degradation during the process of experimental repeater characterization. That is to say the non-self-pulsating laser develops the problem of self-pulsation after lasing for some time. The problem of self-pulsation in this experiment is finally overcome by choosing a laser with low Q cavity (CJ Hwang, personal communication). However, this low Q laser has less power output and causes the dynamic range to be lower than expected.

CONCLUSION

A 0.85- μm fiber optic repeater for radar MTI application is assembled and characterized. This GHz analog repeater has an optical gain of 27.3 and an electrical dynamic range of 42 dB. The minimum detectable optical pulse is measured to be 1.8 μW (or -27.5 dBm) at the repeater output. Output optical pulses with optical power less than 1.8 μW are not detectable because of the presence of the thermal noise associated with the 50 Ω input impedance of the 50-dB amplifier. The other important contribution to the repeater noise is the shot noise associated with the APD detection of the dc biasing optical power. This dc biasing above lasing threshold is needed for a subnanosecond laser response. The noise figure of the repeater is measured to be approximately 6.5 dB (assuming the amplifier A' noise figure to be 4 dB).

The linearity of this repeater is found to be limited by the saturation of non-self-pulsating lasers. These non-self-pulsating lasers are characterized by low Q cavity. The pulse fidelity between input and output optical pulses is examined through subtraction. Typically, the difference between them is 20 dB down compared to either input or output optical pulse.

The frequency response of the repeater is typically flat within ± 2 dB between 10 MHz and 1.3 GHz with non-self-pulsating lasers. The frequency response of lasers with the problems of relaxation oscillation and self-pulsation will peak at a frequency response from 1 to 2 GHz (see fig 11). This nonflatness in frequency response makes the achievement of a GHz analog fiber optic repeater difficult.

The avalanche photodiode (APD) is critically needed in obtaining the minimum detectable output optical pulse of 1.8 μW . An APD provides avalanche gain to the detected optical signal without much degradation in the signal to noise ratio, because the thermal noise associated with the 50 Ω input resistance of the amplifier (see the repeater in fig 1) is the dominant noise source.

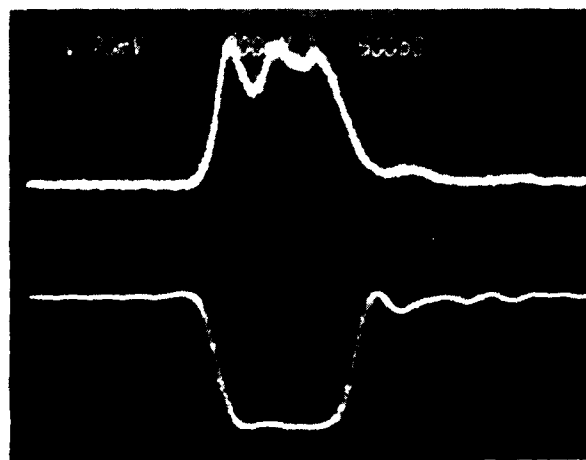
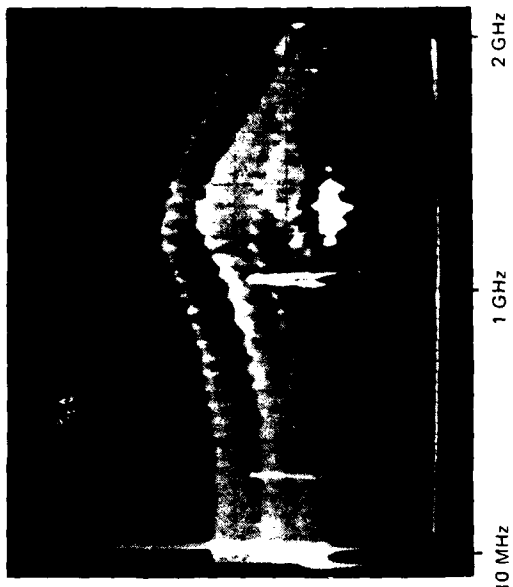
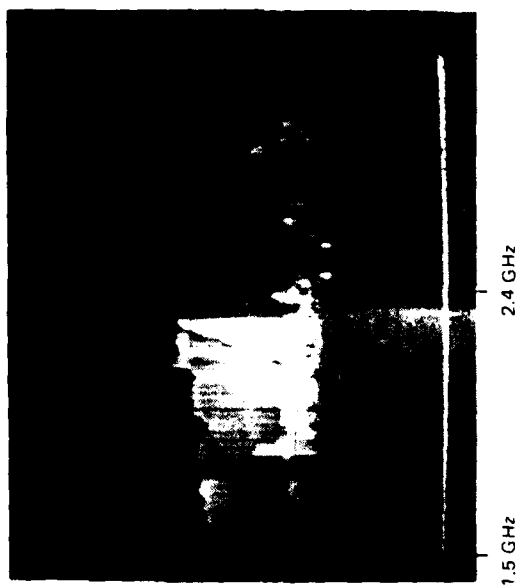


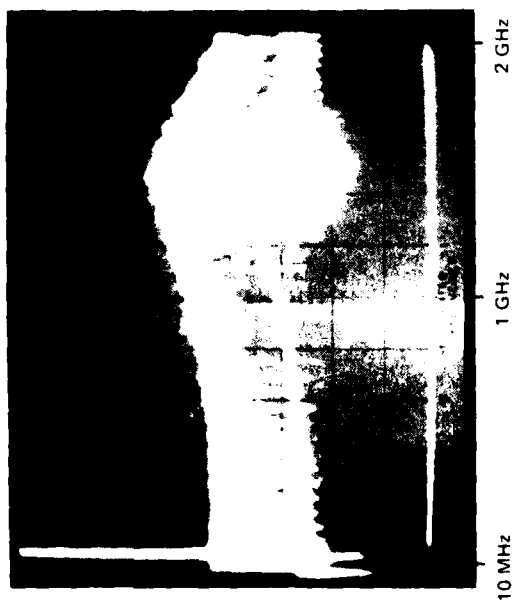
Figure 10. Typical problems in laser diode are (a) self-pulsation, and (b) relaxation oscillation. The detected optical pulse is the bottom trace in (a) and the top trace in (b).



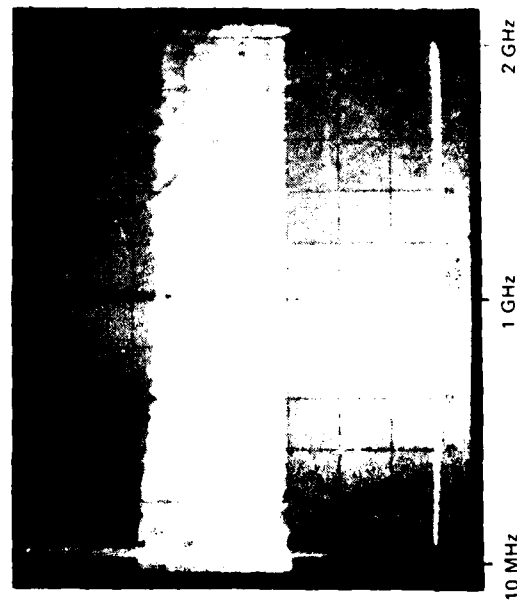
(a)



(b)



(c)



(c')

Figure 11. Frequency response from 10 MHz to 2 GHz of a self-pulsating laser operated at two different dc biasing levels ((a) and (b)). The frequency response of a non-self-pulsating laser is shown in (c) from 10 MHz to 2.0 GHz and in (c') from 1.5 GHz to 2.4 GHz.

The present repeater has an optical gain of 14.4 dB (or 27.3), an electrical dynamic range of 42 dB, and a noise figure of approximately 6.5 dB. This would allow the analog recirculation of a 1-ns pulse through a 5-km fiber with 2.8-dB/km attenuation possible. The signal to noise ratio at the maximum signal amplitude is 30 dB (see fig 7). This is less than 42 dB because of optical signal generated noise (see eq (10)). As a result of the analog noise accumulation in the process of recirculation, the maximum number of analog recirculations will be ~ 2 . After two recirculations the signal to noise ratio will be 17 dB ($\sim 30 - 2 \times 6.5$). This implies that recirculation much more than two times is difficult. In order to achieve a 1-ms delay of a 1-ns pulse, it is necessary to recirculate 39 times through the 5-km fiber optic delay line at 0.85 μm . An alternative method to achieve this long delay (1 ms) is to digitize the radar returns. Digital (binary) transmission can avoid the problem of analog noise accumulation in the repeater.⁴ The regenerated digital signal can be free from the noise, provided that the signal to noise ratio is ≥ 20 dB before the process of digital regeneration.

RECOMMENDATION

It is well known that single-mode fiber attenuation and dispersion are both minimized at the long wavelength region. The best fiber attenuations⁵ reported to date are 0.5 dB/km at 1.3 μm and 0.2 dB/km at 1.55 μm . The single-mode fiber dispersion can also be minimized at these two wavelengths by properly choosing the fiber parameters to obtain cancellation⁶ between material and waveguide dispersions. This long wavelength single-mode fiber with both minimum attenuation and minimum dispersion will be the ideal candidate for wideband radar delay line applications.

Long wavelength double-heterojunction lasers (InGaAsP/InP) are now commercially available. These lasers exhibit high speed modulation capability and high optical output power similar to the 0.85- μm GaAlAs lasers used in this repeater (CJ Huang, personal communication). Ge avalanche photodiodes are the commercially available detectors in the long wavelength region. However, Ge APD is typically noisy because it has a large value of dark current as well as a large excess noise due to avalanche multiplication.⁵ Recently, high performance InGaAlP avalanche photodiodes⁷ have been fabricated. This experimental device has a low dark current ($\sim \text{nA}$) and a low excess noise factor (~ 3 at the avalanche gain of 10).

4. A Yariv, Introduction to Optical Electronics, (C Holt, Reinhardt and Winston, New York, 1976), ch 11

5. T Kimura, Single-Mode Digital Transmission Technology, IEEE Proc 68, 1263-1268 (1980)

6. CT Chang, Minimum Dispersion in a Single-Mode Step-Index Optical Fiber, Appl Opt 18, 2516-2521 (1979)

7. V Diadiuk, SH Groves, and CE Hurwitz, Avalanche Multiplication and Noise Characterization of Low-Dark-Current InGaAsP/InP Avalanche Photodetectors, App Phys Lett 37, 807-810 (1980)

We propose to assemble and to characterize the GHz analog fiber optic repeater operating at the long wavelength region (1.2 - 1.6 μm). If two recirculations of a ns optical pulse through a 5-km fiber with 2.8 dB/km at 0.85 μm are obtainable, then it seems logical to predict that one recirculation of a ns optical pulse through a 25-km long wavelength single-mode fiber with 0.5 dB/km will be successful also. This long wavelength delay line will provide a delay of 250 ns, which is not too far from the required delay time of 1 μs . The worst component in the proposed long wavelength repeater is the avalanche photodiode. The dominant repeater noise (in fig 1) is the thermal noise associated with the 50 Ω input resistance of the amplifier rather than the shot noise from the detector dark current or dc photocurrent. Thus, the nonideal characteristics of long wavelength APD penalize the repeater performance via the excess noise from avalanche multiplication. This excess noise is responsible for the limit of one recirculation through a 25-km long wavelength single-mode fiber as compared to two recirculations through a 5-km single-mode fiber at 0.85 μm .

REFERENCES

1. CT Chang, DE Altman, DR Wehner, and DJ Albares, Noncoherent Radar Moving Target Indicator Using Fiber Optic Delay Lines, IEEE Trans Ckt and Sys CAS-26, 1132-1135 (1979)
2. G Franklin and T Hatley, Don't Eyeball Noise, Elec Dsgn, 24, 184-187 (1973)
3. RG Smith and SD Personick, in Semiconductor Devices for Optical Communication, ed by H Kressel (Springer-Verlag, New York, 1979), ch 4
4. A Yariv, Introduction to Optical Electronics, (C Holt, Reinehart and Winston, New York, 1976), ch 11
5. T Kimura, Single-Mode Digital Transmission Technology, IEEE Proc 68, 1263-1268 (1980)
6. CT Chang, Minimum Dispersion in a Single-Mode Step-Index Optical Fiber, Appl Opt 18, 2516-2521 (1979)
7. V Diadiuk, SH Groves, and CE Hurwitz, Avalanche Multiplication and Noise Characterization of Low-Dark-Current InGaAsP/InP Avalanche Photodetectors, App Phys Lett 37, 807-810 (1980)

ATE
LMED
-8